UNDERSTANDING AND ENGINEERING OF NATURAL SURFACES WITH ADDITIVE MANUFACTURING

Ali Khoshkhoo[1], Andres L. Carrano[4], David M. Blersch[2], Hamid Ghaednia[3], and Kamran Kardel[4]

[1]Department of Industrial and Systems Engineering, Auburn University, Auburn, AL 36849
[2]Department of Biosystems Engineering, Auburn University, Auburn, AL 36849
[3]Department of Mechanical Engineering, Auburn University, Auburn, AL 36849
[4]Department of Manufacturing Engineering, Georgia Southern University, Statesboro, GA 30458

Abstract

Benthic algae systems that attach to substrata have been shown effective in water pollution remediation and biomass production, but yields are limited by attachment preferences in wild cultivars. This work seeks to uncover the surface topography preferences for algal attachment by reproducing natural surface topographies using additive manufacturing. To date, no other research efforts have taken advantage of using additive manufacturing to reverse engineer the characteristics of natural surfaces for enhancement of the attachment preferences of certain periphyton species towards substrata topography. Natural rocks and surfaces with attached biofilms were retrieved from streams, scanned with optical profilometry, and the surface characteristics were analyzed. A material jetting process is used to additively manufacture the surfaces, followed by optical profilometry to validate the resultant topography. The results show that certain texture parameters (e.g., S_{mr}, S_a, and S_v) are significant in affecting the biomass adhesion of specific algal communities.

Keywords: additive manufacturing, reverse engineering, surface metrology, topography, natural surfaces, benthic algae

Introduction

Additive Manufacturing (AM) is a process of creating 3D specimens from a 3D model by adding material layer by layer [1]. The main advantage of AM technologies compared to traditional manufacturing is its capability to fabricate complex geometries with internal features. AM technologies have been used in industries for prototypes, production tools, and multiscale system components [2]. A comprehensive classification of AM processes is described by the ASTM F2792−12a standard [1], which classifies the AM processes in seven categories: binder jetting, directed energy deposition, material extrusion, material jetting, powder bed fusion, sheet lamination, and vat photopolymerization [1]. Material jetting is one of the most recently developed AM technologies. In this technology, a photopolymer resin is repeatedly projected over the tray surface through a printing head and cured by ultraviolet (UV) radiation to form a part. The printing head consists of hundreds of micro-jetting orifices that are capable of forming layers of 16 µm thickness [3], [4].

Algae are a diverse group of photosynthetic organisms that range in size from unicellular genera to multicellular forms which belong to different evolutionary lineage [5]. Due to their fast-

growing rates, high lipid contents, regeneration capabilities, and the potential for water remediation, cultivated algae constitute a promising source of biomass for bio-economic materials. In particular, benthic algae rely on attachment to substrates for colonization and growth. Cultivation of benthic algae in algal turf scrubber (ATS) reactors promises efficient and sustainable water pollution remediation and biomass production while providing ecological services by linking biomass production to aquatic nutrient recovery and carbon capture [6]. Process yields at large scale open ATS systems are limited, however, by competitive exclusion of desired species by wild cultivars, and process control over recruitment, colonization, and growth of desired cultivars is necessary [6]. Engineering the physical and chemical characteristics of the colonized substrate using new materials and approaches promises to advance process control via species management in mixed periphytic communities. Reverse engineering of the natural substrate to understand the underlying surface characteristics that allow specific benthic algae to settle, attach and thrive is fundamental for the development of economically viable cultivation system. Additive Manufacturing (AM) provides precise incorporation of surface topography where surface texture parameters can be controlled to affect the characteristics of the overlying fluid velocity boundary layer, nutrient delivery, and surface contact angle and energy. Since 3-D printing uses a slicing algorithm to layer a solid model, it offers the unique ability to fabricate geometries that are impossible through traditional methods. This work seeks to establish feasibility on the idea of preferential algal attachment based on controlled surface topographies informed by natural substrates that show preferential attachment. Additive manufacturing (3-D printing) is used to enable specific, high fidelity topographical surface features. For this purpose, bare and colonized natural surface specimens were collected from rivers, and their surface topography reversed engineered by 3-D printing to provide artificial substrates with attractive surface characteristics for algal communities.

The primary objective of this effort is to show feasibility in the approach of reverse engineering natural surfaces to enhance the attachment and species selectivity of benthic algae used in water pollution recovery systems. A secondary objective seeks to elucidate the surface parameters that explain the attachment behavior of a particular species.

Materials and Methods

For this purpose, an overview of the reverse engineering methodology proposed in this work is depicted in the general workflow shown in Figure 1. Broadly, a collection of natural rock specimens were retrieved from Chewacla Creek, located in Chewacla State Park, Auburn, Alabama (32°32'51.0"N 85°28'53.7"W) (a), then the colonized and bare (non-colonized) areas were specified and rocks placed in a furnace at the temperature of 575 °C for four hours to burn everything but the rock. Next, the specified areas were analyzed using digital microscopy (b). These areas were scanned with optical profilometry (c and d), and feature characterization method [7] was applied to characterize the significant features (d and e). Surface parameters were extracted and analyzed (f). Based on the surface texture parameters, a surface with matching texture parameters was generated with Matlab® (g), fabricated with 3-D printers (h) and scanned for fidelity of the build. Finally, the printed surfaces are to be placed in the photo-bioreactors for a period, then collected and harvested (i), and analyzed for biomass.

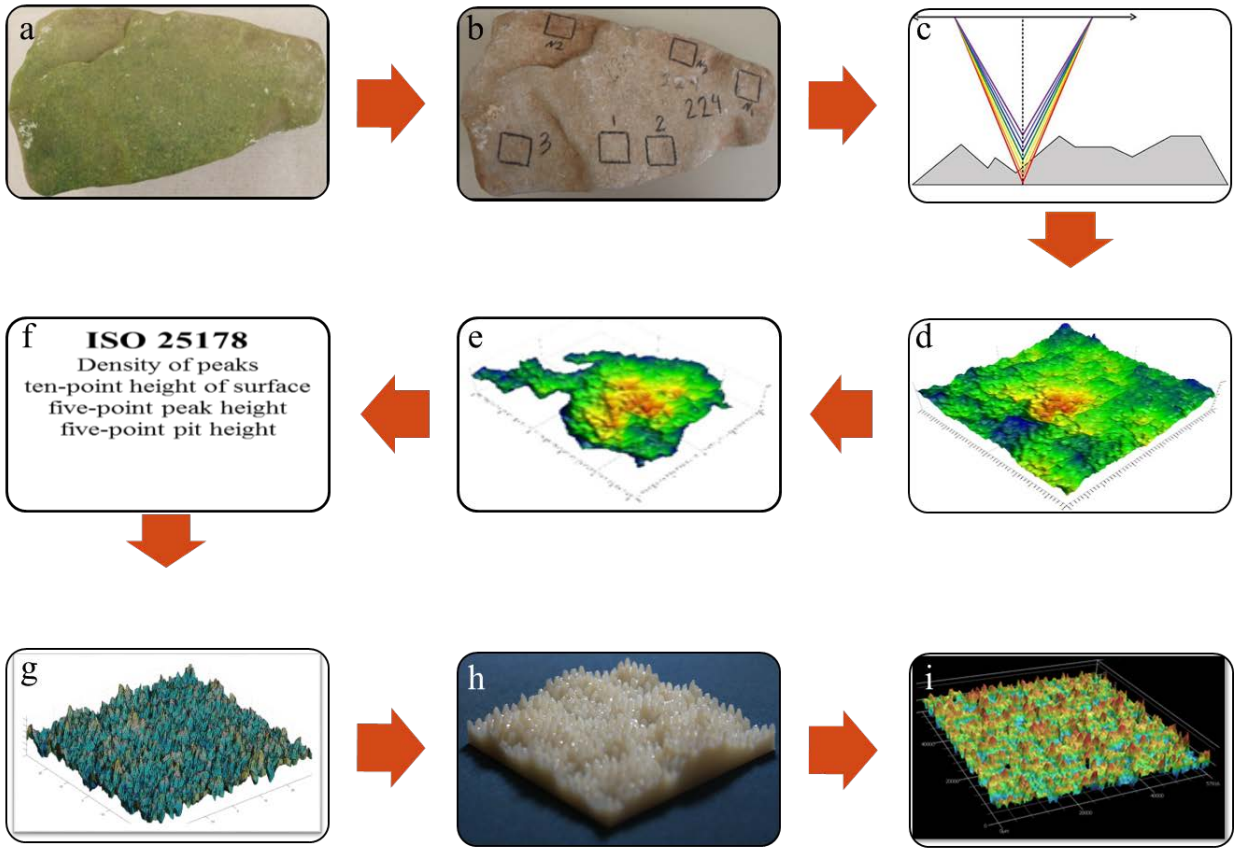

Figure 1: Schematic of the reverse engineering of natural substrata.

With respect to the collection of natural surfaces (a), eleven rock specimens were retrieved. These rock specimens were sought to present areas that would maximize algal attachment contrast (e.g., bare and colonized) contained on a face flat enough such that most topographical features would be within the profilometer scanning range. Several promising areas contrasting various levels of algal attachment were selected and identified immediately after collection. Several areas of 10 mm × 10 mm were identified and marked with graphite. Following standard dry ashing protocols, the rock specimens were placed in crucibles inside a furnace at 575 °F for four hours to burn off all algal matter, bacteria, and any organic matter (b). Figure 2 shows a sample of one of the rock specimens before and after the furnace treatment. The following steps (c, and d) involve scanning the selected areas of 10 mm × 10 mm with a structured light profilometer (VR-3000, Keyence, Osaka, Japan) using a 5 µm step size in both X and Y direction and an acquisition rate of 100 Hz. Those areas where missing points accounted for less than 10% of the total raw data were kept. Although several areas were identified in each specimen surface, those presenting the highest visual contrast, as assessed through micrograph inspection, were selected for this preliminary work. One specimen was deemed unsuitable for reliable scanning and thus discarded in the process. For the remaining ten specimens, the raw data was processed with Mountains®

(Digital Surf, Besancon, France) surface imaging and metrology software and used for parameter calculation and topography imaging (steps e and f),.

Figure 2: Sample of the natural surface before and after furnace treatment (showing target scan sections).

In order to characterize the surface of natural rocks, a set of field and feature parameters are selected for analysis. The field and features parameters comprised a number of different families: height, spatial, hybrid and functional parameters were calculated. Over 30 parameters were studied with the intention of choosing a set of parameters which are functionally correlated to the algal attachment of selected species. The protocol and calculations established by the ISO 25178-2 standard [7] were followed. In order to isolate the relevant surface topography, the waviness and form components were removed using a robust Gaussian filter at 0.8 mm cut-off length. The list of a number of considered parameters with their definitions is presented in Table. 1.

Table 1: Essential areal surface texture parameters to study the surface topography of natural rocks.

Type of parameter	Parameter	Description	Definition
Feature parameters	S_{10z} *(µm)*	the ten-point height of the surface	S_{10z} is the average value of the heights of the five peaks with largest global peak added to the average value of the heights of the five five pits with the largest global pit height.
	S_{5v} *(µm)*	the five point pit height of the surface	S_{5v} is the average value of the heights of the five five pits with the largest global pit height.
Height Parameters	S_q *(µm)*	root mean square height	S_q is the root mean square value of the ordinate values within a defined area.
	S_{sk}	skewness	S_{sk} is the quotient of the mean cube value of the ordinate values and the cube of S_q within a defined area.
	S_{ku}	kurtosis	S_{ku} is the quotient of the mean quartic value of the ordinate values and the fourth power of S_q within a defined area.

	S_p *(µm)*	maximum peak height	S_p is the largest peak height value within a defined area.
	S_v *(µm)*	maximum pit height	S_v is minus the smallest pit height value within a defined area.
	S_z *(µm)*	the maximum height of the surface	S_z is sum of the maximum peak height value and the maximum pit height value within a defined area.
	S_a *(µm)*	arithmetical mean of the absolute of the ordinate values within a defined area	S_a is arithmetical mean of the absolute of the ordinate values within a defined area.
Functional Parameters	S_{mr} *(%)*	the areal material ratio	S_{mr} *(c)* is the ratio of the material at a specified height *c* to the evaluation area.
	S_{mc} *(µm)*	the inverse areal material ratio	S_{mc} *(mr)* is height *c* at which a given material ratio *(mr)* is satisfied.
	S_{xp} *(µm)*	peak extreme height	S_{xp} is the difference in height between the *p* and *q* material ratio.

A preliminary experiment performed with a replicated 3D-printed custom textures were conducted to single out the features (hills or dales) of interest for algal communities. It was observed that that the algal attachment predominated in dales rather than hills as shown in Figure 3. Therefore, dales were selected for segmentation as the features of interest.

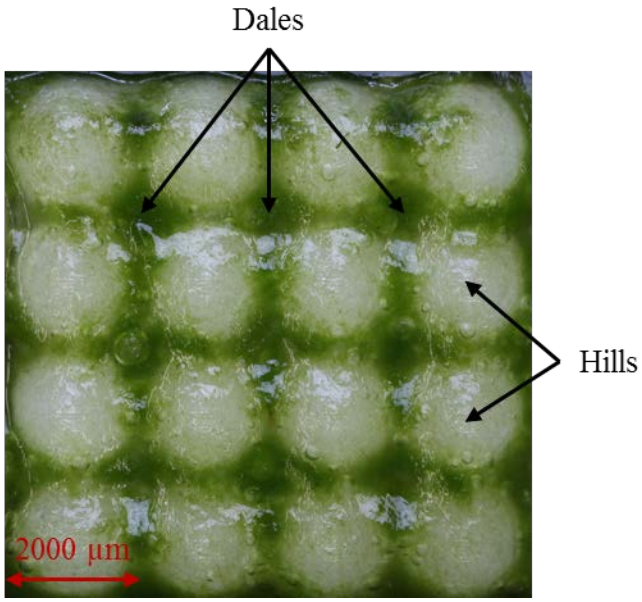

Figure 3: Colonization preference (dales) for benthic algae.

Since the conventional surface texture parameters do not take individual surface features into consideration, and because it has been shown that such features play a significant role in algal colonization, a feature characterization approach was undertaken. This work followed the 5-step feature characterization (steps e and f) established in ISO 25178-2 consisting of: (I) selection of

the type of texture feature, (II) segmentation, (III) determination of significant features, (IV) selection of feature attributes and (V) quantification of feature attribute statistics. Wolf pruning [7] was the approach used for pattern recognition and segmentation of significant and non-significant surface topographies. Since Wolf pruning produces different counts of features at various thresholds, the recommended 10% of S_z (maximum height of the surface) value was used as the thresholds for features. This pruning of the data retained all data elements above the 10% watershed value thus deemed significant. An additional area prune was applied if, through software calculation, a dale was found to represent less than 3% of the total area. After that, the remaining features were selected and extracted, and the parameters were calculated on those features. This feature recognition and segmentation as performed in one of the specimens is illustrated in Figure 4.

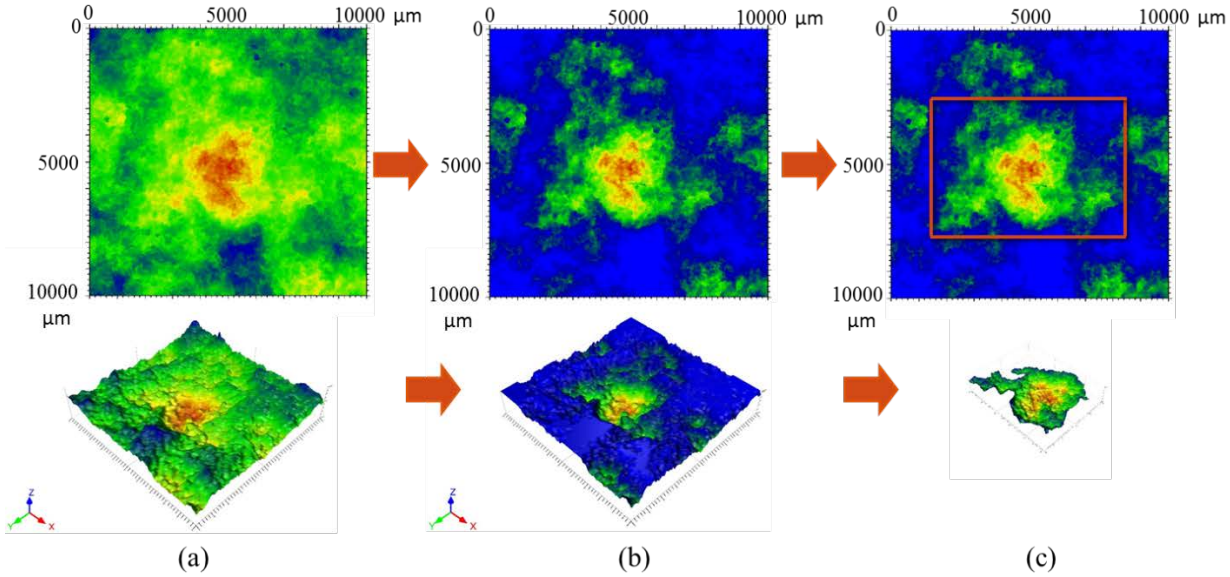

Figure 4: Wolf-pruning: (a) original surface, (b) Wolf pruning 10% Sz; (c) significant feature (dales) extraction.

Statistical paired t-tests on the difference between the means of colonized and non-colonized dales were performed. Table 2 presents the surface texture and significant features' (dales) parameters, mean of parameters of colonized features and areas, standard deviation of parameters of colonized features and regions (σ colonized), mean of parameters of non-colonized features and regions, the standard deviation of parameters of non-colonized features and regions (σ non-colonized). The p-value column represents the results of t-tests of each parameter for colonized features with 26 samples and non-colonized features with 24 samples features and regions. Among all these parameters, areal material ratio (S_{mr} *(%)*, p-value=0.000, α = 0.05), the maximum pit height (S_v, p-value=0.015, α = 0.05), arithmetical mean of the absolute of the ordinate values (S_a, p-value=0.026, α = 0.05) were found significant. The S_{mr}, Eq. (1), is the areal material ratio (expressed as a percentage) of the cross sectional area of the surface at a certain height relative to the evaluation cross sectional area. The S_v is the lowest point found on the surface and the S_a, Eq. (2), indicates significant deviations in the texture characteristics. Figure 5 shows the scatter plots of the significant parameters. As it can be seen in Figure 5, areal material ratio

separates the colonized and non-colonized areas. Therefore, the S_{mr}, $S_{v,}$ and S_a are chosen for reverse engineering of natural surfaces.

$$S_{mr} = \left(\frac{A(m)}{A(N)}\right) \times 100 \tag{1}$$

$$S_a = \frac{1}{A}\iint_A |z(x,y)|dxdy \tag{2}$$

Where, *A*, is the area of the measured surface, *Z (X, Y)*, is the height at the point *(X, Y)*, *A (m)*, is the area of the cross sectional area of the surface at mean height, *m*, and *A (N)*, is the evaluation cross sectional area.

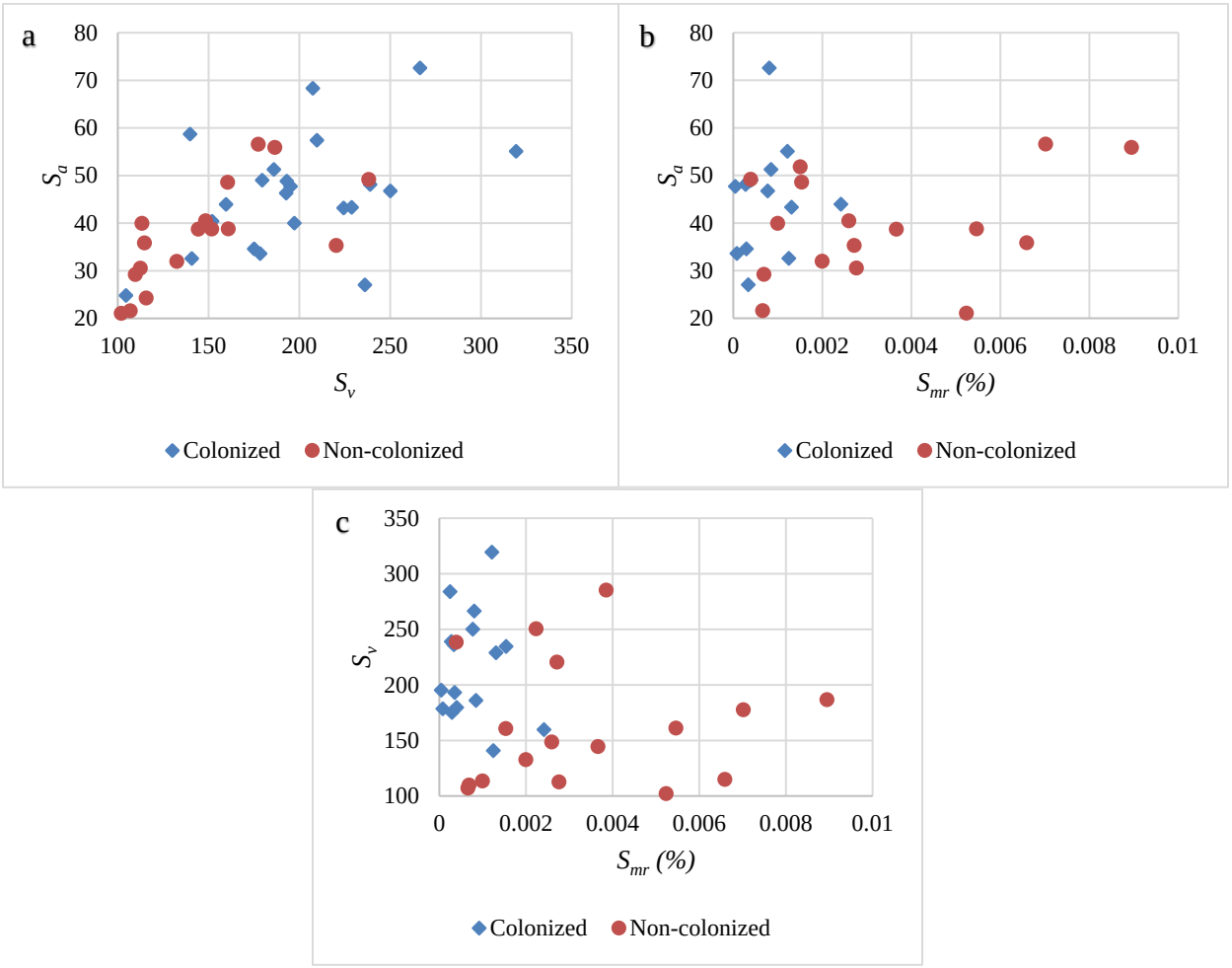

Figure 5: Preliminary results. Scatter plots of significant parameters.

Table 2: Surface texture and significant features' (dales) parameters of colonized and non-colonized areas.

Type of parameter	Parameter	Description	Mean colonized	σ colonized	Mean non-colonized	σ non-colonized	p-value
Feature Parameters	S_{10z} *(µm)*	the ten-point height of the surface	430.9	95.9	441.9	174.8	0.633
	S_{5v} *(µm)*	five-point pit height	217.7	50.2	234.9	127.3	0.832
Height Parameters	S_q *(µm)*	root mean square height	59.2	15.8	50.3	17.0	0.085
	S_{sk}	skewness	-0.2	0.5	-0.3	0.4	0.663
	S_{ku}	kurtosis	2.7	0.3	2.8	0.5	0.581
	S_p *(µm)*	maximum peak height	207.2	91.3	192.6	75.6	0.542
	S_v *(µm)*	maximum pit height	203.9	49.1	163.6	55.8	0.015
	S_z *(µm)*	the maximum height of the surface	424.9	114.8	367.4	147.3	0.136
	S_a *(µm)*	arithmetical mean of the absolute of the ordinate values	46.6	12.0	38.2	10.9	0.026
Functional Parameters	S_{mr} *(%)*	areal material ratio	0.0008	0.0007	0.0040	0.0020	0.000
	S_{mc} *(µm)*	inverse areal material ratio	87.8	41.3	104.7	55.2	0.224
	S_{xp} *(µm)*	peak extreme height	133.0	49.1	115.4	46.5	0.222

The modeling and reverse engineering steps (g and h) consisted of generating and fabricating the irregular surfaces with the specified S_{mr}, S_v and S_a values obtained from the bare and colonized areas of the selected rocks. For this purpose, a Pearson continuous probability distribution function is used to generate surfaces (step g) with the targeted surface roughness properties [8]–[10]. The Pearson's systems of frequency curves are capable of generating a density function with given roughness properties if its first four moments are known, i.e., the mean, standard deviation, skewness, and kurtosis [10]. The Pearson distribution can generate a surface with precise, targeted first four moments values approaching the specific texture parameters from the targeted surface [10]. Since the density functions in this study are nondimensionalized, they are only dependent of skewness and kurtosis of the surface. The parameter k is presented in Eq. (3) to identify the type of curve [11].

$$k = \frac{S_{sk}^2(S_{ku}+3)^2}{4(2S_{ku}-3S_{sk}^2-6)(4S_{ku}-3S_{sk}^2)} \quad (3)$$

Where S_{sk} and S_{ku} denote the skewness and kurtosis of surface, respectively. The parameter, *k*, ranges from -∞ to +∞. Based on the value of *k*, the appropriate equation of the density function is selected. The equations and types of the probability density function (pdf) using the Pearson system of frequency curves are presented in Table 3.

Table 3: Equations and types of the probability density function (pdf) using the Pearson system of frequency curves [10], [11]**.**

Type number	**Equations with origin at the mean**	**criterion**
I	$\varphi^*(Z^*) = y_0\left(1+\frac{Z^*}{A_1}\right)^{m_1}\left(1-\frac{Z^*}{A_2}\right)^{m_2}$	$-\infty < k < 0$
II	$\varphi^*(Z^*) = y_0\left(1-\frac{Z^{*2}}{a^2}\right)^{m}$	$k = 0, S_{sk} = 0, S_{ku} < 3$
III	$\varphi^*(Z^*) = \frac{1}{\sqrt{2\pi}}e^{\left(-\frac{z^{*2}}{2}\right)}$	$k = 0, S_{sk} = 0, S_{ku} = 3$
IV	$\varphi^*(Z^*) = y_0\left(1+\left(\frac{Z^*}{a}-\frac{v}{r}\right)^2\right)^{-m} e^{-vtan^{-1}\left(\frac{Z^*}{a}-\frac{v}{r}\right)}$	$0 < k < 1$
VI	$\varphi^*(Z^*) = y_0\left(1+\frac{Z^*}{A_1}\right)^{-q_1}\left(1+\frac{Z^*}{A_2}\right)^{q_2}$	$1 < k < \infty$
VII	$\varphi^*(Z^*) = y_0\left(1+\frac{Z^{*2}}{a^2}\right)^{-m}$	$k = 0, S_{sk} = 0, S_{ku} > 3$
The parameters, $y_0, A_1, A_2, m_1, m_2, a, r, v, m, q_1, q_2$ that used in these equations depend on the skewness and kurtosis [11].		

The skewness and kurtosis values for both colonized and bare areas approximately are -0.3 and 3 (close to the values in a normally distributed surface) respectively. Thus, the skewness and kurtosis values for the reverse engineered surfaces were kept as -0.3 and 3.0 respectively. With the assumed skewness and kurtosis values, the criterion *k*, which designates the density function types, is calculated (-0.256, Type I). The S_v value for the generated surface can be targeted by multiplying the variable, *h* with the pseudo random numbers generated by the Pearson function. The S_a values can be obtained by changing the standard deviation of the pseudo random numbers. In order to further control the S_{mr} values, micro-patterned depressions (circular holes) are superimposed to the simulated surfaces. These patterns help approach specific S_{mr} values for the generated surfaces.

In order to fabricate a pseudo random surface with specific parameters, the following steps were performed in Matlab®:

a) Calculate the parameter *k*, Eq. (3), to determine the type of Pearson distribution.
b) Specify S_a: generate pseudo random numbers with specific values for the first four moments (i.e., mean, variance, skewness, and kurtosis) of the Pearson distribution. A surface with specific S_a value can be reached with different combinations of the four moments.
c) Mesh the points in *X* and *Y* direction to create a surface.
d) Allocate the generated numbers to each point in *X* and *Y* direction.
e) Specify the S_v: multiply the random numbers to a variable, *h*, to magnify them in the *Z* direction. Multiply the variable *h* changes the height of the asperities (features) that directly affect the S_v.
f) Convert a thin surface to a closed triangulated solid volume. This step helps to change the surface model to a manufacture-able solid model.
g) Specify the S_{mr}: create circular depressions (hole) patterns on the surface to change the material ratio of the surface. The frequency and size of the depression patterns reduce the material ratio of the surface.
h) Generate the *.STL* format file from surface data.
i) Fabricatethe part.

In order to validate the proposed reverse engineering method, two levels for S_{mr}, $S_{v,}$ and S_a parameters have been chosen. The detailed information of the levels is presented in Table 4. Figure 6 shows the profilometry images of these two levels.

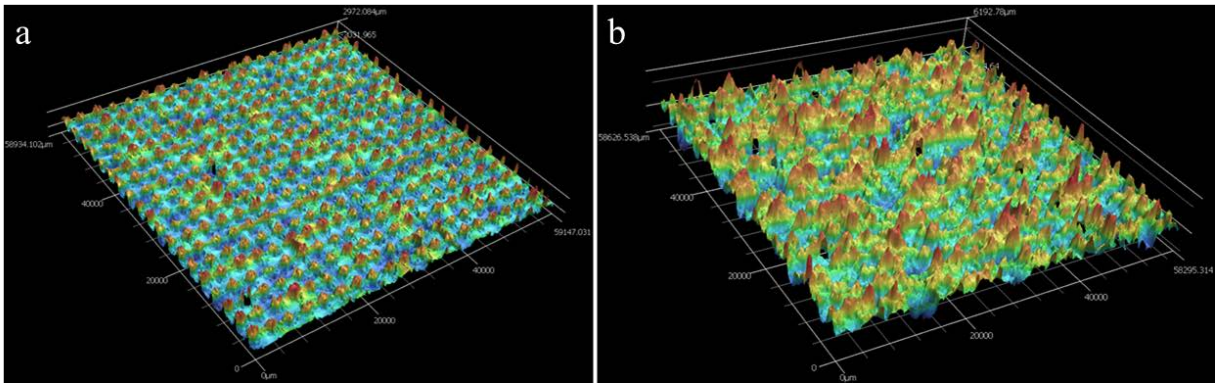

Figure 6: Profilometry images of fabricated specimens for level 1 (a) and level 2 (b)

Table 4: Experimental design factors and levels.

Factors	Control mechanism	Level 1	Level 2
S_{mr},	**Controlling S_{mr} with generating micro-patterned depressions on surface**	Without micro-patterned depressions $\sim S_{mr1} \sim$ 50%	With micro-patterned depressions $\sim S_{mr2} \sim$ 37%
S_v	**Reversed engineering based on S_v**	S_{v1}=3.4 mm	S_{v2}= 6.6 mm
S_a	**Reversed engineering based on S_a**	S_{a1}= 0.7 mm	S_{a2}= 1.3 mm

Three replicates were considered for each treatment for a total of six acrylic polymer reversed engineered surfaces (60 mm × 60 mm × 3 mm) were modeled by the Pearson distribution in Matlab® and fabricated (Figure 7) with an Objet30 3D (Stratasys Ltd., Eden Prairie, MN) printer (step h) with a 28 µm layer thickness. The accuracy of the build verified with optical methods using a structured profilometer (VR-3000, Keyence, Osaka, Japan) with 20 nm resolution in the vertical direction. Figure 7 shows the areal map and the 3D profile of the surface topography of the reverse engineered surface.

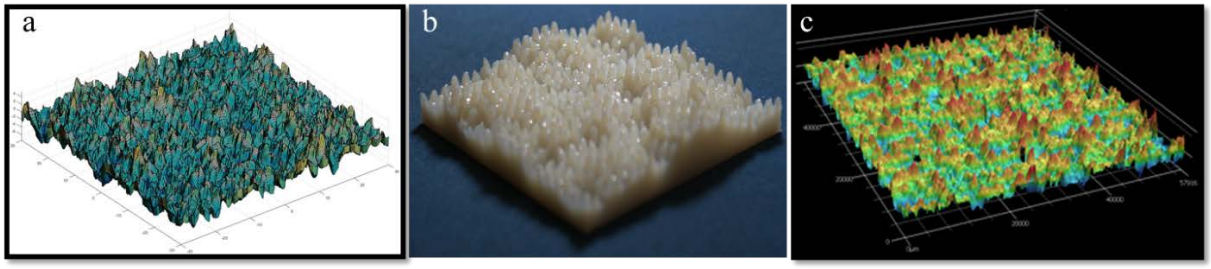

Figure 7: Computer model (a), reverse engineered surface (b), and scanned image (c).

Once the model has been fabricated with the material jetting process, the samples are scanned with the optical profilometer to measure the accuracy of the process. Eight surface parameters were examined to test the fidelity of the method, (i.e., S_{mr}, S_p, S_{ku}, S_{sk}, S_z, S_q, S_a, and S_v).

Results and Discussion

Figure 8 and Table 5 present the error percentage (the deviation of actual measured value from the targeted value of computer model) of the eight parameters that are calculated for the computer model and measured from scanned data. The description and definition of each parameter presented in Table 5. The results show that the S_{mr} has the lowest average percentage error and the S_a, and S_v have the largest errors among others.

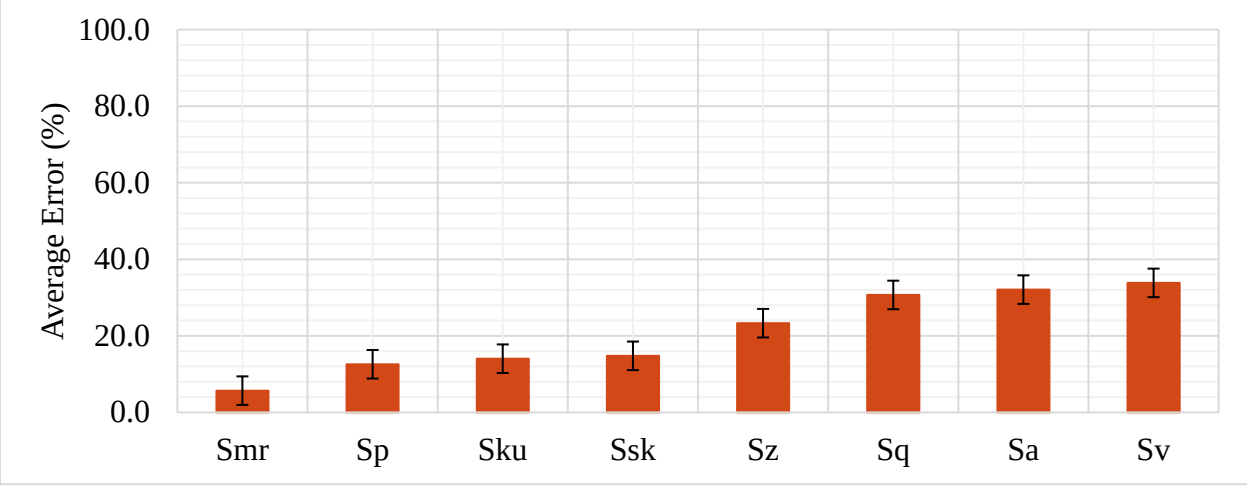

Figure 8: Average error of targeted surface texture parameters of a computer model from scanned surfaces.

Table 5: Summary of measured and calculated data for computer model and scanned surfaces.

Parameter	Actual data	Designed data	Average Error (%)
S_{mr} (%)	43.9	42.5	5.7
S_p (µm)	4362.1	5165.9	12.6
S_{ku}	3.4	3.0	14.0
S_{sk}	0.6	0.5	14.8
S_z (µm)	7635.9	10198.4	23.3
S_q (µm)	904.5	1312.4	30.7
S_a (µm)	706.8	1044.5	32.1
S_v (µm)	3273.8	5032.5	33.8

One interpretation of the results can be obtained by comparing the resolution of the computer model and the additive machine. The resolution of computer models was set at 100 µm in X and Y direction. In addition, based on the obtained results it is hypothesized that the accuracy of the printer machine is various depending on features aspects such as size, geometry, etc.

To validate the hypothesis and to find the resolution of the machine, a preliminary experiment designed and performed by fabricating a prototype in three replicates with four different feature designs (i.e., spherical and square hole and protrusions) with various length sizes ranged from 25 µm to 1600 µm and height sizes ranged from 12.5 µm to 800 µm (Figure 9). A subsequent experiment was performed to test the resolution and accuracy of the machine for different geometries in various sizes. The dimensional accuracy of the machine is measured with a white light profilometer (ST-400, Nanovea, Irvine, California) with a resolution of 5µm in X and Y direction.

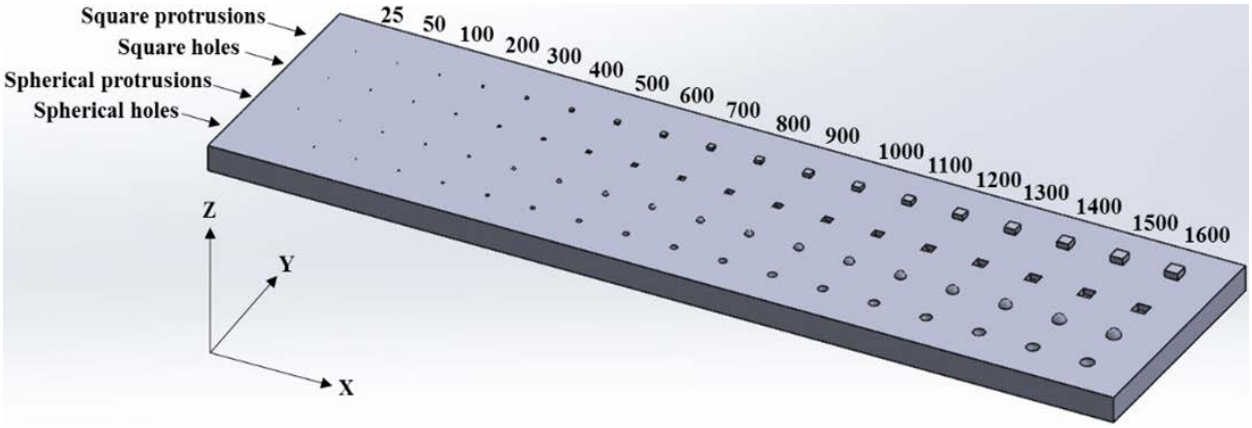

Figure 9: A Computer model of a designed prototype for testing dimensional fabrication error.

Figure 10 indicates that the protrusion features are fabricated with higher fidelity, presenting smaller error than hole features, especially in small sizes (< [700 µm-length and 350 µm-height]). This can be a reason for why the parameter S_p than S_v has higher error percentage. This shows that the accuracy of the machine is higher when printing the hills (average error 12.5%) than the dales (average error 33.8%) as shown in figure 10.

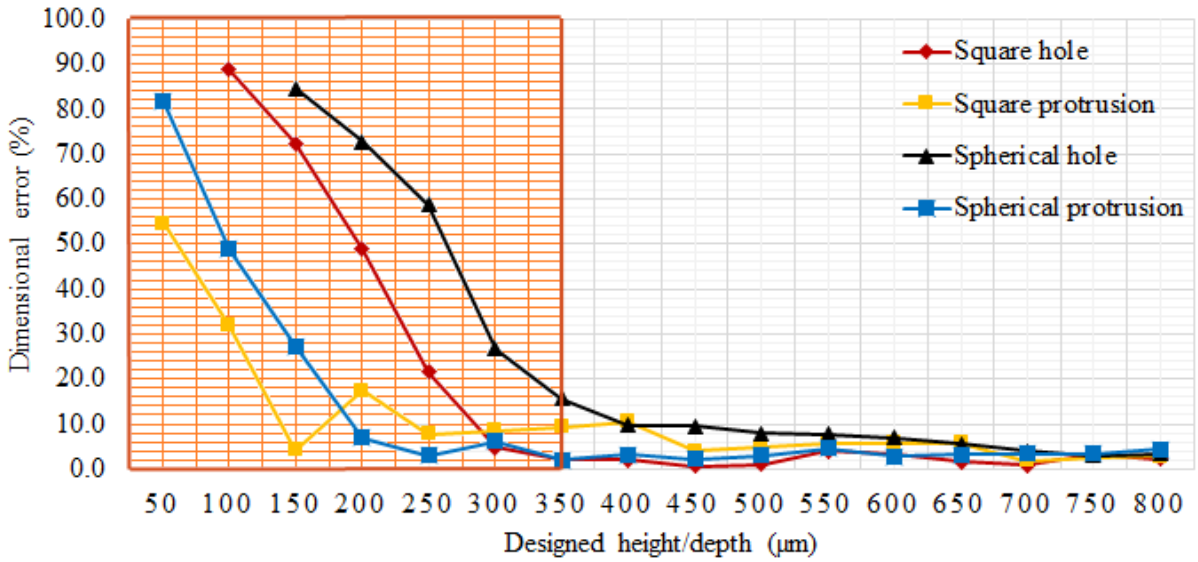

Figure 10: Dimensional fabrication error by type of asperity.

The S_{mr} is more robust (average error < 6%) compared to other parameters because it is dependent more on lower frequency signals (waviness) than the higher frequency roughness of the surface (Figure 11). By limitation of the printers, it should be easier to reproduce the waviness profile than features in the roughness scale.

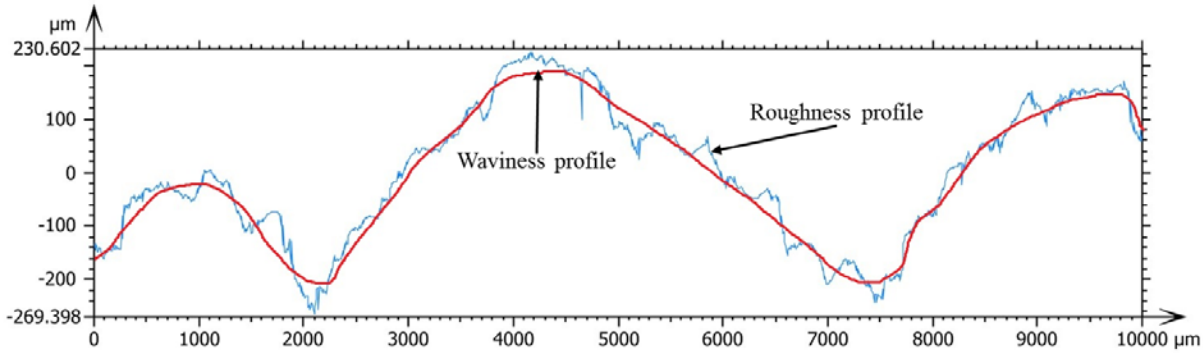

Figure 11: Waviness profile and roughness profile of a scanned rock.

Conclusion

This work sought to reveal the surface topography parameters that were significant for algal attachment by manipulating surface topographies using additive manufacturing. In this study, a method for capturing and reversing natural substrata has been developed and proven feasible. Natural rocks and surfaces with attached biofilms were retrieved from streams, scanned with

optical profilometry, and the surface characteristics were analyzed. The results show that certain texture parameters (e.g., S_{mr}, S_a, and S_v) show promise in predicting surface colonization by algae. The Pearson distribution was utilized to generate pseudo randomized surfaces with surface characteristics. A material jetting process was used to additively manufacture the surfaces followed by optical profilometry to validate the resultant topography.

Surface metrology parameters (i.e., S_{mr}, S_p, S_{ku}, S_{sk}, S_z, S_q, S_a, and S_v) are utilized to test the fidelity of the proposed method. The results showed that the accuracy of metrology parameters are varied depending on the resolution of the machine in different axes. Among selected metrology parameters for validation process, S_{mr} had a lowest average error (5.7 %), while S_v and S_a had the highest average error (33.8 %). The precision of the additive machine was lower than the computer model which causes the error in reverse engineering method.

A preliminary experiment performed to test the manufacturability of the material jetting process. It was observed that designed sharp peaks become smooth curves after fabrication which affects the S_v and S_a parameters the most. The S_{mr} was more robust compared to other parameters since it is dependent on waviness rather than roughness profile. Future work will focus on higher fidelity of the reproduction of the surface topography as well as validation of algal attachment with photo-bioreactors.

References

[1] American Society for Testing and Materials Committee F42 on Additive Manufacturing Technologies, "Standard terminology for additive manufacturing technologies," ASTM International, 2012.

[2] A. Cazón, P. Morer, and L. Matey, "PolyJet technology for product prototyping: Tensile strength and surface roughness properties," *Proceedings of the Institution of Mechanical Engineers, Part B: Journal of Engineering Manufacture*, vol. 228, no. 12, pp. 1664–1675, Dec. 2014.

[3] K. Kechagias J., P. Stavropoulos, A. Koutsomichalis, I. Ntintakis, and N. Vaxevanidis, "Dimensional accuracy optimization of prototypes produced by polyjet direct 3d printing technology," presented at the Advances in Engineering Mechanics and Materials, 2014, pp. 61–65.

[4] N. Beltrán, F. Carriles, B. J. Álvarez, D. Blanco, and J. C. Rico, "Characterization of factors influencing dimensional and geometric errors in polyjet manufacturing of cylindrical features," *Procedia Engineering*, vol. 132, pp. 62–69, 2015.

[5] R. J. Stevenson, M. L. Bothwell, R. L. Lowe, and J. H. Thorp, *Freshwater Benthic Ecosystem*. Algal ecology, 1996.

[6] Andres L. Carrano, David M. Blersch, Kamran Kardel, and Ali Khoshkhoo, "Understanding attachment preferences of benthic algae through controlled surface topographies on 3D-printed substrata," presented at the 5th International Conference on Surface Metrology, Poznan, Poland, 2016.

[7] 25178-2 ISO, "Geometrical product specifications (GPS) — Surface texture: Areal — Part 2: Terms, definitions and surface texture parameters," 01-Apr-2012.

[8] Stout, K. J., "The Pearson system of distributions: its application to non-gaussian surface metrology and a simple wear model," *Journal of Lubrication Technology*, p. 495, Oct. 1980.

[9] C. A. Kotwal and B. Bhushan, “Contact Analysis of Non-Gaussian Surfaces for Minimum Static and Kinetic Friction and Wear,” *Tribology Transactions*, vol. 39, no. 4, pp. 890–898, Jan. 1996.
[10] N. Tayebi and A. A. Polycarpou, “Modeling the effect of skewness and kurtosis on the static friction coefficient of rough surfaces,” *Tribology International*, vol. 37, no. 6, pp. 491–505, Jun. 2004.
[11] W. P. Elderton and N. L. Johnson, “Systems of frequency curves,” *CERN Document Server*, 1969. [Online]. Available: http://cds.cern.ch/record/109766. [Accessed: 01-Mar-2017].